3D SOUND INTENSITY VARIABILITY IN SHALLOW WATER IN PRESENCE OF INTERNAL WAVES IN SWARM'95 EXPERIMENT

MOHSEN BADIEY[1)], BORIS KATSNELSON[2)], JAMES LYNCH[3)],
SERGUEY PERESELKOV[2)], WILLIAM SIEGMANN[4)]

[1)] University of Delaware
Newark, DE 19716, USA
mbadiey@Udel.edu

[2)] Voronezh State University
Universitetskaya sq.1, Voronezh 394006, Russia
katz@phys.vsu.ru

[3)] Woods Hole Oceanography Institute
Woods Hole, MA 02543, USA
jlynch@whoi.edu

[4)] Renseller Polytechnical Insitute,
Troy, NY 12180 USA
siegmw@rpi.edu

Broadband shot signal data are analyzed from the SWARM'95 experiment to investigate acoustic variability in presence of internal solitons. A 10 to 15 minute temporal variations in the intensity of the received signals were observed. These temporal variations are azimuthally dependent on variability of water column in the presence of internal solitary waves. These fluctuations should be explained by significant horizontal refraction (3D-effects) taking place when orientation of acoustic track is close to direction of the wave front of internal solitons. Analysis on the base of both equation of vertical modes/horizontal rays and PE in horizontal plane is carried out, good agreement between theoretical calculations and experimental data is obtained.

INTRODUCTION

Generation of most of internal waves (IW) in shallow water regions is due to tidal forcing interaction with topographical features. When the water depth becomes shallow at the

continental shelf, the difference of water depth causes a hydraulic jump condition in which solitons packets can be generated and will propagate shoreward. This will create an inhomogeneous anisotropic medium in which the acoustic waves can propagate. When broadband acoustic waves transmit through these internal wave packets, they go through an amplitude and phase fluctuation elated to the characteristic of the solitons. Quantifying the interaction between these two types of waves is of interest in bath fields of underwater acoustics and shallow water oceanography.

1. SWARM'95 EXPERIMENT

The goal of the SWARM'95 experiment was to quantify the effects of water column and ocean bottom inhomogeneities on acoustic transmission in shallow regions. This experiment was con- ducted in the Mid-Atlantic Bight on the continental shelf region off the coast of New Jersey (see Fig. 1). Several research vessels participated in the experiment including R/V Oceanus, R/V Hatteras and R/V Endeavor. Principal investigators in the project included researchers from the Naval Research Laboratory (NRL), Woods Hole Oceanographic Institution (WHOI), the University of Delaware (UD), and the Naval Postgraduate School. Many oceanographic measuring systems as well as two vertical line arrays (VLA) were deployed to conduct experiments in which the acoustic and detailed environmental data were collected simultaneously [2]. We will consider here part of this experiment dealing with WHOI vertical array. The WVLA, positioned at 39°14.25'N, 72°54.55'W, consisted of 16 elements and spanned the water column from 14.9 m to 67.4 m, with hydrophone spacing of 3.5 m, and used a sampling rate of 1395Hz. Five temperature sensors were also attached to the array at 12.5, 22.5, 30.5, 50.5 and 60.5m below the sea-surface. Studied propagation track was designed by UD and WHOI [1] to emphasize on the azimuth dependence of the acoustic field due to the horizontally anisotropic propagation environment in this shallow water region. in Fig. 1 an observed internal wave front is also marked as dotted straight lines. Bathymetry is an important factor affecting the acoustic transmission. Our surveys and archival data indicated that the propagation path from the UD source station to the WVLA has a nearly flat bottom

During the experiment various environmental sensors were deployed in support of the acoustic measurements. The R/V Endeavor performed high resolution oceanographic surveys using Conductivity- Temperature-Depth (CTD) casts and tows, an Acoustic Doppler Current Profiler (ADCP), and high-frequency (200 & 300 kHz) sonars for imaging internal waves. These measurements were used for characterizing the generation, dispersion, and decay of the internal wave and background fields. These environmental data were supplemented with CTD data acquired by the Oceanus, Hatteras, and other internally-recording oceanographic instrumentation moorings. The latter included two moored ADCP units, six thermistor arrays, and internally recording temperature sensors distributed over the two acoustic receiving arrays. During these experiments, both direct observations and the satellite images indicated strong internal wave activities occurring over a large region in the experiment site.

To show the variations in internal wave activity, a 2 hour (Aug. 4, 1995) segment of the temperature data is shown in Fig. 2. These are temperature profiles from two thermistor sensors close to the thermocline located on the WHOI receiver array (at about 22.5 m and 40.5 m from the sea-surface respectively). For this period the mixed layer depth is about 15 m and the negative temperature gradient extends from 15-30 m. The fluctuations of the thermocline

shown for this period indicate a change in the sound speed from about 1535 m/s above the thermocline to 1480 m/s below the thermocline. It is noticed that both the depth and the thickness of the surface mixed layer changes with time. Below the thermocline, temperature has much less variation, indicating a nearly isovelocity water column. The period of the temperature fluctuations shown in the selected segment is about 10 to 15 minutes. We refer to these fluctuations as short-term compared to the longer period (on the order of 10 hours) fluctuations associated with tidal forcing. Although not shown in here, similar features are also found in data collected from other temperature sensors at different sites including at source location

2. ACOUSTIC MEASUREMENTS

Throughout the experiment, two different acoustic source signals were transmitted from Hatteras every minute. One was an air gun source (duration 0.1 s) and the other was a Linear-Frequency-Modulated (LFM) sweep (duration 30 s) generated by a J-15 transducer. These sources' signatures were highly repeatable. Signature of airgun and its spectrum is shown in the Fig.3.

Stayed at fixed location for several hours, both sources (air gun and LFM sweep) fired acoustic signals continuously. During interval 18:00 to 20:00 GMT on August 4, 1995, the sources were at location shown in Fig. 1. This source location was about 15 km from WVLA. For this time period, the airgun was placed at 12m below the sea-surface (above the thermocline). A sixty-minute segment acoustic data from 19:00 to 20:00GMT is shown in Fig. 4. Signals were transmitted every 60.038 sec.

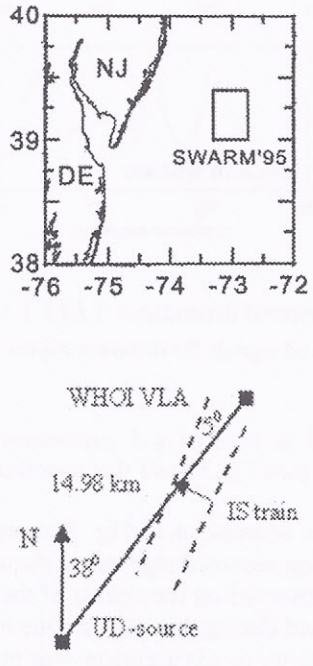

Fig.1. Layout of the SWARM'95 experiment

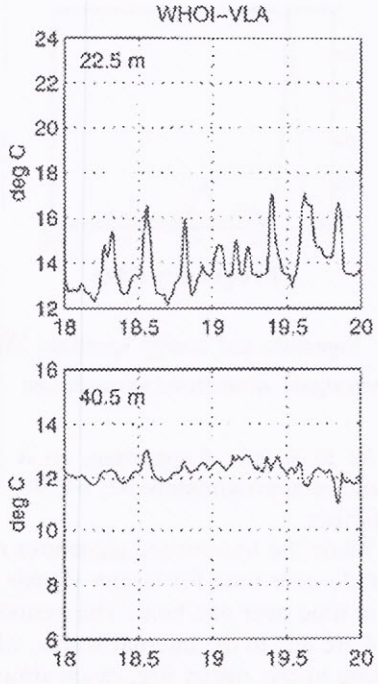

Fig.2. Temporal behavior of temperature at the point of receiver for two depths

Let it have radiated signal (or strength of source) $f(t)$ with the spectrum:

$$S(\omega)=\frac{1}{2\pi}\int_{-\infty}^{\infty} f(t)e^{i\omega t}dt \qquad (1)$$

Total energy per pulse is:

$$E_0=\frac{1}{4\pi\rho c}\int_{-\infty}^{\infty} f^2(t)dt=\frac{\pi}{\rho c}\int_{0}^{\infty}|S(\omega)|^2 d\omega \qquad (2)$$

Estimation of the power of source with duration of pulse ~ 0.1 sec, amplitude of the sound field at the distance 2 m ~ 15 kPa gives source level 210 dB with respect to 1μPa at 1 m

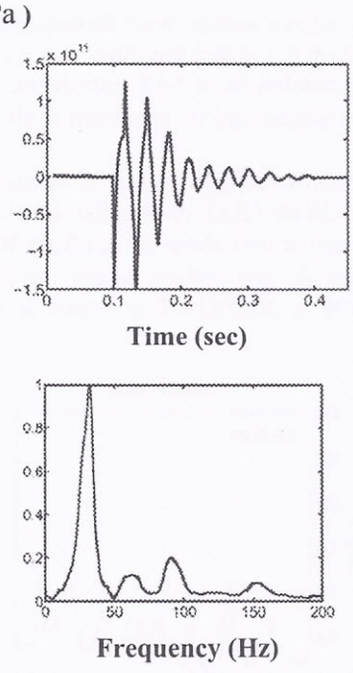

Fig 3. Signature and energy spectrum $|S(\omega)|^2$ of airgun signal normalized to maximum

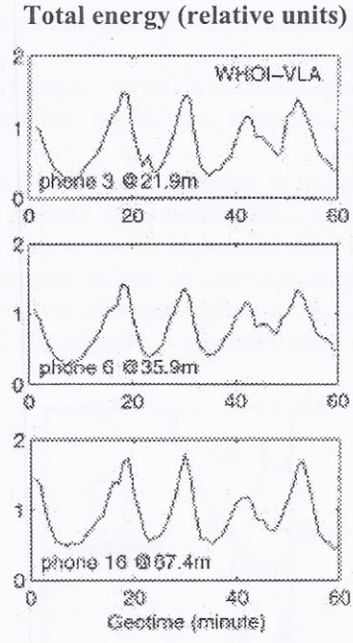

Fig.4 Temporal dependence ($E(T)$) of energy of received signals for different depths

As to shape of spectrum, so it can be presented as sum of 4-5 harmonics with the frequencies approximately 32, 64, 96, 128 and 160 Hz (see Fig.3) and this spectrum will be used further.

While the transmitted signatures measured near the sources, as in Fig. 3, show constant amplitude over time for airgun signals, the corresponding received signatures show modulations in time over one hour. The periodic fluctuations observed on the arrival of the spikes in Figs. 4 are due to the internal waves, which were observed during this period. Due to the bubble pulse in the airgun fire, much stronger signal sensitivity to environment was observed in airgun data than in the LFM sweep data. To further quantify the internal wave effect on

acoustic transmission, we focus mostly on the airgun sweep data in this study. WVLA signals show strong fluctuations in amplitude versus geotime, indicating acoustic dispersion due to a more developed internal soliton packet along the path from the source to the WVLA. Although the variations of the signal in geotime do not exactly correspond to the precise time and location of the internal waves based on the shipboard observations for this period (see Fig. 2), they have the same periodicity

A quantitative representation of the acoustic intensity variation (or more exactly total acoustic energy per pulse) is calculated from:

$$E(\bar{r},z;T) = \int_{T}^{T+\Delta t} \frac{|p|^2}{2\rho c}\, dt \qquad (3)$$

where Δt is duration of received pulse (~0.1 sec), T is geotime (since 19 till 20 hours) or in relative units since 0 till 60 min.

This dependence on geotime for different depths of hydrophones was measured during 60 min and is shown in the Fig.4.

Let's list the following features of presented fluctuations, requiring special explanation:

1) Significant amplitude of fluctuations (up to 3-4 dB). This value cannot be explained by local displacement of thermocline level. Rough estimation of intensity fluctuation, conditioned by changing of the sound speed profile due to thermocline displacement, give 10-15% variation of received intensity
2) Synchronicity in depth . We can observe that fluctuations at different depths re practically the same, even fluctuations increase near the bottom
3) Correlation with IW oscillations, more over, minimum in sound intensity (as a function on IW position) takes place if receiver is at the point with minimal value of temperature (minimal value of the sound speed comparatively nearest area in horizontal plane)

Our main idea is that listed peculiarities can be interpreted as manifestation of horizontal refraction in sound propagation (in other words) as manifestation of 3D effects.

3. MODEL OF SHALLOW WATER CHANNEL WITH INTERNAL WAVES

In order to model this experiment let's introduce the following model of the sound channel. Acoustic track of the length 15 km with the flat bottom (depth $H = 70$ m) has sound speed profile $c(\bar{r},z)$, taken from experimental data, and bottom with the sound speed $c_1 = 1600$ m/sec, $\rho_1 = 1.8$ and attenuation coefficient $\alpha \approx 0.1$ dB/λ. Here $\bar{r} = (x,y)$ is radius vector in horizontal plane.

Dependence on horizontal coordinate is conditioned by internal waves. X-axis is parallel to wave front of IW which is supposed to be plane, IW propagate in negative direction of Y-axis with the velocity ~0.55 m/sec (see Fig.5), shape of IW, corresponding to temperature record if one and the same at the source and receiver. In accordance with experiment acoustic track is directed at angle ~ 5° with X-axis and position of the source and receiver are placed at different wave fronts of IW.

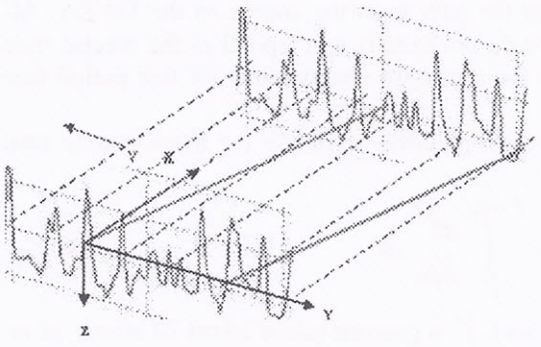

Fig.5 Model of acoustic track. Left solid straight Denotes acoustic tack at 19-00, right straight Line will occupy position of acoustic track at 20:00

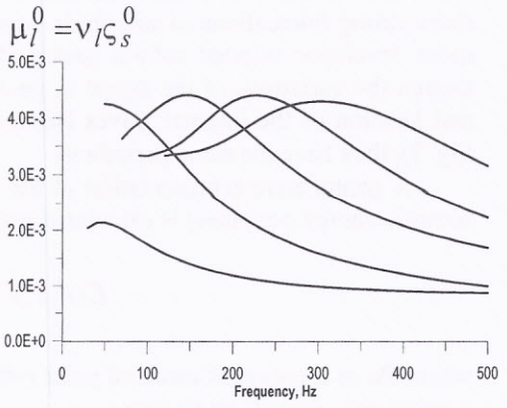

Fig. 6 Frequency dependence of effective refractive index for HR for five lowest VM

Straight lines in horizontal plane denote position of our acoustic track: left one corresponds to the 19-00 geotime, the right one corresponds to 20-00. Source is placed at the point $\vec{r}_s = 0, z_s$

In given paper we analyze temporal and depth dependence of the total intensity (energy) of the sound pulses. For this we consider initially separate Fourier components $\Psi(\vec{r}, z; \omega)$ of the sound pressure at the point of observation $\vec{r}, z$, in other words the Green function, satisfying the following equation:

$$[\nabla^2 + k^2(\vec{r}, z)]\Psi(\vec{r}, z; \omega) = -\delta(\vec{r} - \vec{r}_s)\delta(z - z_s) \qquad (4)$$

where $k(\vec{r}, z) = \omega / c(\vec{r}, z)$ - wave vector, containing perturbation, depending on space-coordinates. If, as usually, we will find Green function as expansion in series over eigen function, time depending comlex signal $p = \mathrm{Re}\, P$ at the point of observation has the form:

$$P(\vec{r}, z, t) = 2\int_0^\infty S(\omega)\Psi(\vec{r}, z; \omega)e^{-i\omega t}d\omega = 2\int_0^\infty S(\omega)\sum_l \psi_l(\vec{r}; z)P_l(\vec{r})e^{-i\omega t}d\omega \qquad (5)$$

where $\psi_l(\vec{r}, z)$ are adiabatic (vertical) modes (VM) or eigen functions of the corresponding Sturm - Liuoville problem, depending on horizontal coordinates as on parameters , complex eigen numbers are $\xi_l = q_l + \gamma_{l/2}$. For the total sound energy flux for the pulse (energy per unit of square) at the point of observation we have result after averaging over some frequency interval $\delta\omega$. If $\delta\omega \sim \omega\Lambda / r$, where Λ is ray cycle, then terms remain only with $l = m$ and spectral density of the sound intensity:

$$E(\vec{r}, z) = \frac{2\pi}{\rho c}\int_0^\infty d\omega |S(\omega)|^2 \sum_l |P_l(\vec{r})|^2 \psi_l^2(z) \qquad (6)$$

So the main calculated value is $P_l(\vec{r})$. Let's substitute (2) into (1) and neglecting the mode coupling we get equations for the modal amplitudes $P_l(\vec{r})$:

$$\left[\partial^2/\partial x^2 + \partial^2/\partial y^2 + \xi_l^2(\vec{r})\right]P_l(\vec{r}) = 0 \qquad (7)$$

4. DISTRIBUTION OF THE SOUND FIELD IN HORIZONTAL PLANE. HORIZONTAL RAYS AND VERTICAL MODES

Equation (7) should be considered as 2-D Helmholtz equation, which can be solved in different ways. First of all we can formulate 2-D ray approximation (or theory of the so called "horizontal" rays (HR)). Let's find function $P_l(\vec{r})$ in the form

$$P_l(\vec{r}) = \sum_n A_{nl}(\vec{r})\exp[i\theta_{nl}(\vec{r})] \qquad (8)$$

Here $A_{nl}(x,y)$ - amplitude, $\theta_{nl}(x,y)$ - eikonal for l-th vertical mode $\psi_l(\vec{r};z)$, depending on horizontal coordinates as on parameters. Remark, that in general case several HR, corresponding to given mode, can reach point of observation. These rays have different trajectories, therefore, they are characterized by different amplitudes and eikonals. Due to this circumstance in (8) we carry out summation over horizontal rays too (index n).

For amplitude and eikonal we can get ordinary (2-D) equation of ray acoustics:

$$(\nabla_r\theta_{nl})^2 = q_l^2(\vec{r}), \qquad (9)$$

$$2\nabla_r A_{nl}\nabla_r\theta_{nl} + A_{nl}\nabla_r^2\theta_{nl} + q_l\gamma_l A_{nl} = 0\,. \qquad (10)$$

Ray trajectories in horizontal plane can be found from the ordinary differential equations:

$$\frac{d\vec{r}_{nl}}{dt} = U_l\vec{\tau}_{nl}\,,\quad \frac{d\vec{q}_{nl}}{dt} = U_l\nabla q_l \qquad (11)$$

where $dt = U_l^{-1}\sqrt{(dx)^2+(dy)^2}$, $\vec{\tau}_{nl}(\vec{r}) = \nabla_{\vec{r}}\theta_{nl}(\vec{r})/|\theta_{nl}(\vec{r})|$ - unit vector in horizontal plane, tangent to horizontal ray, $\nabla_\perp = \nabla_{\vec{r}} - \vec{\tau}(\vec{\tau}\nabla_{\vec{r}})$ - gradient in transverse direction, $U_l = (dq_l/d\omega)^{-1}$ is the group velocity of the l-th vertical mode, $\vec{q}_{nl} = q_l\vec{\tau}_{nl}$ - wave vector, tangent to n-th ray, corresponding to l-th vertical mode.

Remark, that equations (11) describe the so-called space-time horizontal rays [3]. Using these equations we can find not only trajectories of horizontal rays, but arrival times for the corresponding modal pulses. These equations should be accompanied by initial conditions at the point of source $\vec{r}_s = (x_s, y_s)$, so:

$$\vec{r}_l(t;\vec{r}_s,\vec{\tau}_s)\big|_{t=0} = \vec{r}_s\,,\ \vec{q}_l(\vec{r}_l,t;\vec{r}_s,\vec{\tau}_s)\big|_{\vec{r}_l=\vec{r}_s,t=0} = \vec{q}_{ls} = q_l(x_s,y_s)\vec{\tau}_s \qquad (12)$$

where $\vec{\tau}_s = (\cos\chi_s, \sin\chi_s)$, χ_s is horizontal output angle from the source. For fixed point of the source χ_s and t can be considered as ray coordinates: if we fix χ_s we get separate horizontal ray, for fixed t we have wave front in horizontal plane, or curve line in the plane. In three-dimensional space it corresponds to cylindrical surface. If we know rays, we can construct eikonal function:

$$\theta_l(\vec{r},t) = \theta_l(\vec{r}_s,0) + \int_0^t U_l q_l[\vec{r}(t')]dt' \qquad (13)$$

Here integration is carrying out along ray.

Because space scale of q_l in horizontal plane is $q_l / \nabla_r q_l$ this value must be much greater than wavelength what provides applicability of presented theory of HR. Amplitude of HR also can be presented:

$$A_l(t) = A_l(0)/\sqrt{J}\exp\left\{i\theta_l(\vec{r},t) - \int_0^t \gamma_l[\vec{r}(t')]/2dt'\right\} \qquad (14)$$

where $J(t)$ denotes divergence of horizontal rays, or ratio of cross sections of ray tube.

For horizontal rays it is ratio of lengths corresponding pieces of wave fronts $J(t) = d\Sigma_l / d\Sigma_0$. So amplitude of the sound field at the receiver can be estimated if we know "density" of rays in horizontal plane or value of cross section. In other words we can estimate intensity of the sound field at the point of receiver. Let's suppose that we have set of rays emitted from the source with equal intervals between output angles. These rays form some ray structure in horizontal plane and due to horizontal refraction these rays do not propagate alone radii directions. For fixed time wave front in horizontal plane is not a circle and rays split this curvilinear wave front onto different pieces. Lengths of these pieces between adjacent rays describe redistribution of the sound intensity in horizontal plane.

Let's construct model for description of the sound propagation in shallow water in presence of IS train. Let' suppose that presence of IS provides some perturbation of the sound speed profile, which in equilibrium state is supposed to be depending on z only. This perturbation will depend on horizontal (transverse) coordinates and time. Remark that dependence on time is supposed to be sufficiently smooth, so we will consider time as parameter. Squared refractive index ($n = c_{ref} / c(\vec{r},z,t)$, where c_{ref} is some fixed value) is:

$$n^2(\vec{r},z,t) = n^2(z) + \mu(\vec{r},z,t) \qquad (15)$$

We can see that dependence on horizontal coordinates different with the effective squared refractive index, conditioned by internal solitons (waves)

$$\mu(\vec{r},z,t) = -2\delta c(\vec{r},z,t)/c(z) = -2QN^2(z)\zeta(\vec{r},z,t) \qquad (16)$$

where $N(z) = \left(gd\rho / \rho dz\right)^{1/2}$ is Vaisala frequency, $Q \sim 2.4$ m^2/s, $\zeta(\vec{r},z,t)$ is space-time dependence of the surface of a constant density (isodensity surface):

$$\zeta(\vec{r},z,t) = \Phi(z)\zeta_s(\vec{r} - \vec{u}t)$$

where $\Phi(z)$ is the first gravitational mode, normalized by $\max(\Phi) = 1$, $\zeta_s(\vec{r} - \vec{u}t)$ is envelope of IS train, $\vec{u} = (u_x, u_y)$ is speed of IS train in horizontal plane.

In the right side of eikonal equation (9) we have effective squared wave vector in horizontal plane. Instead of it we can introduce effective refraction index in horizontal plane:

$$n_l(\vec{r}) = q_l(\vec{r}) / q_l^0,$$

depending on mode number. Similar to (13) it can be presented as a sum of unperturbed value 1 and perturbation, conditioned by IS:

$$n_l^2(\vec{r}) = 1 + \mu_l(\vec{r}) \qquad (17)$$

Correction, conditioned by IS can be found using perturbation theory:

$$\mu_l(\vec{r}) = \frac{1}{(q_l^0)^2}\int_0^H \left[\psi_l^0(z)\right]^2 k^2 \mu(\vec{r},z)dz = \nu_l \varsigma_s(\vec{r}), \qquad (18)$$

where we separate factor ν_l, depending on waveguide parameters and function ζ_s, determined by shape of IS train. Remark, that refraction index in horizontal plane depends also on frequency through frequency dependence of eigen function. More exactly, frequency dependence of refraction index in horizontal plane is determined those fact, that overlapping integral (18) depends on what part of eigen function is placed in the thermocline area. In the Fig.6 value $\mu_l^0 = \nu_l \zeta_s^0$ is shown, characterizing value of refraction index when IS amplitude is 10 m.

We can see that structure of refraction index in horizontal plane repeats structure in IS, it meansalso is similar to diffraction grating structure.

If, for example $h_t / H \sim 0.2$, $N_0 \sim 15c/h \sim 0.026 s^{-1}$ then $\nu_l \approx -6.2 \cdot 10^{-4} m^{-1}$ and correction to the squared refraction index in horizontal plane is $\mu_l(\vec{r}) \sim -6.2 \cdot 10^{-4} \zeta_s(\vec{r})$, what corresponds to values, presented in the Fig.6.

Let's estimate sector of angles, for horizontal rays having turn point within the region between adjacent wave fronts. Using simple ray assertions it can be estimated in our case $\chi_0 \sim 2\sqrt{\nu_l \zeta_0} \sim 10^\circ$. Remark, that it is lower boundary, due to our estimation of the value of eigen function within thermocline layer. Further let's estimate maximal scale of focusing (one half of ray cycle in horizontal plane for rays with horizontal deviation of the order $\Lambda/2$).

$$X_0 = \int_0^y \frac{dy}{tg\chi(y)} = \int_0^{\Lambda/2} \frac{dy}{\sqrt{\nu_l \zeta_s(y)}} \sim \frac{2\Lambda}{\chi_0} \tag{19}$$

If $\Lambda \sim 400 m$, $\zeta_0 \sim 10\ m$, then $X_0 \sim 4 km$. It means the our "critical region" can be placed within the sector with central angle χ_0 and for distances greater than X_0. We can remark, that our experimental position of source and receiver allows us to wait influence of horizontal refraction on the sound field.

This structure of refraction index in horizontal plane can lead to focusing/defocusing of horizontal rays [5] in dependence on position of the source relative internal waves. In other words in dependence on position of the receiver we will observe increasing or decreasing of the sound field. In the Fig.7 we show results of calculations of HR structure for two times 19-14 and 19-22 corresponding to maximum and minimum in the time dependence of sound intensity (Fig.3)

5. PE IN HORIZONTAL PLANE AND INTENSITY SPACE-TIME DISTRIBUTION

In order to explain the last results let's consider sound field at the receiver for the fixed frequency as a function of geotime T: $\Psi(\vec{r}, z; \omega, T)$ and as a function of position of the source. Let' s introduce factor $P_l^0(\vec{r}_r, \vec{r}_s; T)$ to describe horizontal refraction in "pure" form:

$$\Psi(\vec{r}, z; \omega, T) = \sum_l \psi_l(0, z_s) \psi_l(\vec{r}, z) P_l^0(\vec{r}, \vec{r}_s; T) e^{-\frac{\gamma_l}{2}|\vec{r} - \vec{r}_s|} \tag{20}$$

here $\vec{r}_s, \vec{r}$ are coordinates of the receiver and the source in horizontal plane, z_r, z_s are depths of the receiver and the source, γ_l - attenuation coefficient of the l-th mode. This form allows us to understand modal distribution in horizontal plane. In order to get real energy distribution we should multiply by modes excitation coefficients at the depth of the source and the receiver, and take into account modal attenuation along the acoustical track.

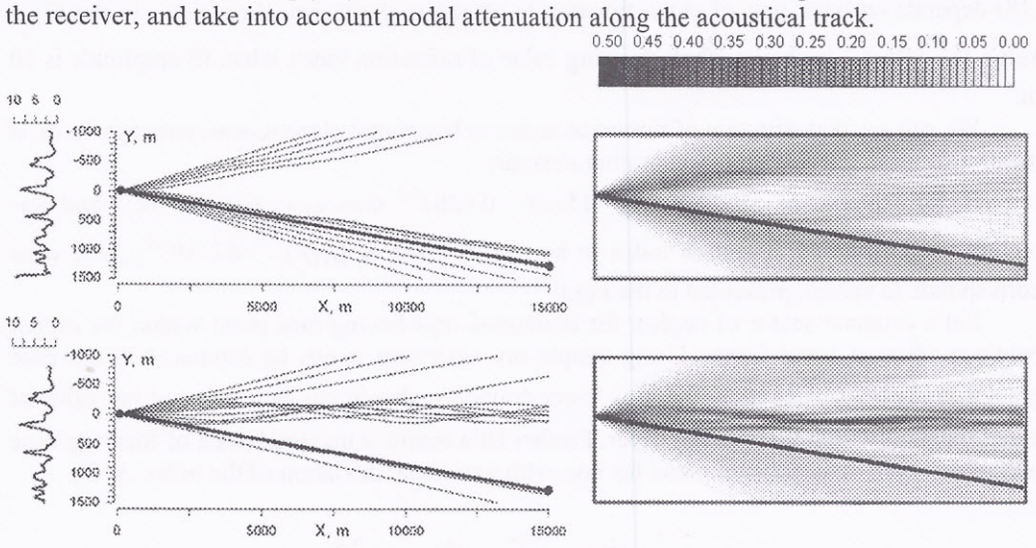

Fig.7 Ray (left part) and PE (right part) pictures in horizontal plane, corresponding to GMT 19-14 (upper picture- defocusing of HR and maximum in sound field energy) and 19-22 (lower picture - focusing of HR and minimum in energy) . In the left part we show position of IW, corresponding to given GMT. Bold straight lines denote acoustic track.

For calculations of the sound field it is worth to use PE equation in horizontal plane to avoid ordinary problems of ray acoustics, connected with problem of caustics etc. In this case solution of (7) is presented in the form

$$P_l^0(\vec{r}) = F_l(x,y)\exp\left[iq_l^0 x\right] \tag{21}$$

where $F_l(x,y)$ is slowly varying function of longitudinal coordinate. For $F_l(x,y)$ in forward scattering approximation ($\partial F_l/\partial x << q_l^0 F_l$) we cam get PE in horizontal plane:

$$\frac{\partial F_l}{\partial x} = \frac{i}{2q_l^0}\frac{\partial^2 F_l}{\partial y^2} + \frac{iq_l^0}{2}\mu_l F_l, \tag{22}$$

Numerical solution of this equation can be produced using standard method connected with Fourier transform. Spectral intensity can be calculated from formula:

$$I(\vec{r},z;\omega,T) = \frac{1}{2\rho c}\sum_l \psi_l^2(0,z_s)\psi_l^2(\vec{r},z)\left|P_l^0(\vec{r},\vec{r}_s;T)\right|^2 e^{-\gamma_l|\vec{r}-\vec{r}_s|} \tag{23}$$

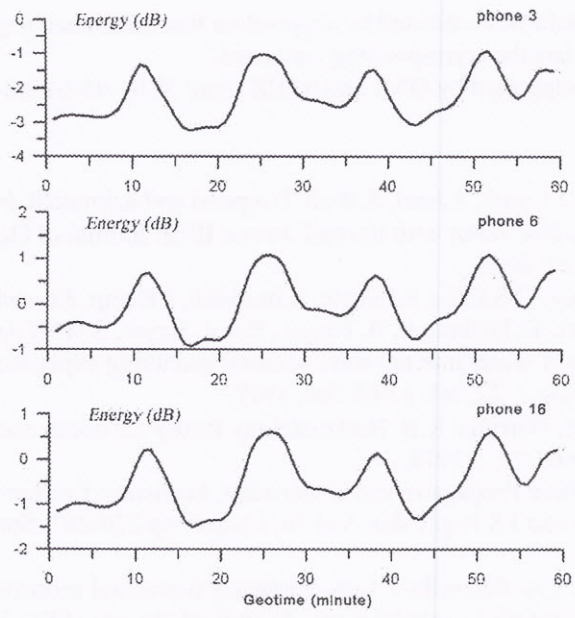

Fig.8. Temporal dependence of energy of pulses, calculated according to presented theory.

Total energy can be obtained by summation of intensities for different frequencies. In this way we have result for temporal behavior of total energy

$$E(\vec{r},z;T)=\frac{2\pi}{\rho c}\int_0^\infty |S(\omega)|^2 I(\vec{r},z;\omega,T)d\omega \qquad (24)$$

Results of calculation according to formula (24) are shown in the Fig.8 for different depths, corresponding to position of hydrophones in the Fig.4. We can see that there is rather good agreement between experimental (Fig.4)and theoretical data (Fig.8).

6. CONCLUSION

So as a result of presented paper we show temporal dependence of total energy of received signals (Fig.8). On the base of comparison of these results with experimental data (Fig.4) we can see existence of main peculiarities listed in chap.2: amplitude of fluctuations, their synchronicity over depth, and correlation with internal waves confirm our hypothesis about 3D genesis of these phenomena. However upon a closer view we can find small mismatch between theory and experiment. We mean that amplitude of fluctuation is a little less (by 1-2 dB) and temporal dependence (Fig.8) is a little shifted in time (by 3-5 min) in comparison with measured data. We explain this mismatch by significant idealization in our theoretical model. In the first degree it is concerned with supposition about plane wave front of IW and exact repetition of shape of IW at the point of the source (remind that temperature record Fig.2 is made at the point of the receiver only). Of course also there is some uncertainty in angle between wave front of IW and direction of acoustic track and velocity of IW (by the way it was also measured at the point of receiver). It is interesting to note, that both men-

tioned mismatches could be eliminated by supposition that mentioned angle is about 4^0 or that the wave front of IW has the corresponding curvature.

This work was supported by ONR and RFBR grant № 03-05-64568-a

REFERENCES

1. M.Badiey, Y.Mu, J.Lynch, J.Apel, S.Wolf Temporal and azimuthal dependence of sound propagation in shallow water with internal waves. IEEE Journal of Oceanic Engineering, v.27, N1, p.117-129, 2002.
2. J.R.Apel, M.Badiey, C-S.Chiu, S.Finette, R.headrick, J.Kemp, J.Lynch, A.Newhall, M.Orr, B.Pasewark, D.Tielburger, A.Turgut., K.v.d. Heydt, S.Wolf An overview of the SWARM 95 shallow water internal wave acoustic scattering experiment, IEEE Journal of Oceanic Engineering, v.22, N3, p.465-500, 1997.
3. H. Weinberg R.B. Barridge R.B. Horizontal ray theory for ocean acoustics. J. Acoust. Soc. Am. v.55, pp.63-79 , 1974.
4. F.D. Tappert in Wave Propagatio and Underwater Acoustics: Lecture Notes in Physics., Ed. By J.B.Keller and J.S.Papadakis Vol.70, Chap.5, pp 224-287, Springer, New York, 1977
5. B.G. Katsnelson , S.A. Pereselkov Low-frequency horizontal acoustic refraction caused by internal wave solitons in a shallow sea. Acoustical physics, 2000, V.46, N6, pp.774-788, 2000